FRACTURE CHARACTERIZATION OF CELLULOSE FIBER GYPSUM COMPOSITE SUBJECT TO INPLANE TENSION LOADING

CHARAKTERISIERUNG DES BRUCHVERHALTENS EINES CELLULOSEFASER-GIPS-VERBUNDWERKSTOFFS BEI ZUGBEANSPRUCHUNG IN PLATTENEBENE

CARACTÉRISATION DE RUPTURE D'UN COMPOSITE À BASE DE FIBRES CELLULOSIQUES ET DE PLÂTRE SOUMIS À UN CHARGEMENT DE TRACTION

Simon Aicher, Rüdiger Finn

SUMMARY

Cellulose fiber gypsum boards represent a short fiber composite material class which has gained considerable importance as a structural component in building industry in recent years. The non-combustible material is frequently used for bracing in timber frame construction. One of the most interesting features of the material consists in it´s pronounced strain softening behaviour at inplane tension loading where damage localizes at an early loading stage in a crack band.

It is reported on first results of uniaxial tension tests aiming at a direct determination of several fracture softening properties. The strains were measured localized by means of a laser extensometer. Results are given for the strain dependent localization onset, the width of the zone of distributed micro cracking (crack band width), the softening modulus and fracture energy. Further on, fracture energy determined by localized strain measurement is compared to the result obtained from evaluation of global strain measurement.

ZUSAMMENFASSUNG

Cellulosefaser-Gipsplatten repräsentieren einen Kurzfaser-Verbundwerkstoff, der in den vergangenen Jahren eine erhebliche Bedeutung als Material für tragende Zwecke im Bauwesen erfahren hat. Der nicht brennbare Werkstoff wird häufig zur Schubaussteifung im Holzrahmenbau eingesetzt. Eine der inte-

ressantesten Eigenschaften des Materials besteht in dem ausgeprägt dehnungsentfestigenden Verhalten, wobei sich die Schädigung frühzeitig in einem Schädigungsband lokalisiert.

Der Aufsatz berichtet über erste Ergebnisse von einachsigen Zugversuchen zum Zweck der direkten Ermittlung mehrerer Bruch- sowie Entfestigungseigenschaften. Die Dehnungen wurden ortsaufgelöst mittels eines Laser-Extensometers gemessen. Die vorgestellten Ergebnisse umfassen den dehnungsabhängigen Lokalisierungsbeginn, die Breite der Zone der verteilten Mikrorissbildung (Rissbandbreite), den Entfestigungsmodul und die Bruchenergie. Die mittels ortsaufgelöster Dehnungsmessung bestimmte Bruchenergie wird mit dem Ergebnis zufolge globaler Dehnungsbestimmung verglichen.

RÉSUMÉ

Les panneaux à base de fibres cellulosiques et de plâtre constituent un composite à renforts fibreux courts qui a pris ces dernières années une importance considérable comme composant structural en Génie civil. Ce materiau non inflammable est fréquemment utilisé comme élément de chaînage dans les constructions à ossature bois. Une des caractéristiques les plus intéressantes du matériau est son comportement adoucissant très prononcé en traction dans le plan, où l'endommagement se concentre à un stade précoce dans une bande fissurée.

Cet article présente les premiers résultats d'essais de traction uniaxiale visant à déterminer plusieurs caractéristiques d'endommagement adoucissant. Les déformations ont été mesurées au moyen d'un extensomètre laser. Les résultats présentés concernent l'amorce de la localisation des déformations, la largeur de la zone micro-fissurée, le module adoucissant et l'énergie de rupture. Par la suite on compare l'énergie de rupture mesurée par la déformation locale à celle quantifiée par la déformation macroscopique.

KEYWORDS: Fiber gypsum board, short fiber composite material, strain softening, damage zone, strain localization, fracture energy, crack band model

1. INTRODUCTION

Fiber gypsum boards represent a very specific type of short fiber composite materials. The plate type material consists of recycled paper fibers and a matrix material of gypsum. The fiber volume fraction is in the range of about 17 – 20%. The material is a technically superior substitute for the brittle gypsum wall board and excelled especially by two features, being incombustible and showing pronounced strain softening, i.e. damage tolerance [1-3]. At present, a comprehensive research project, funded by German Research Foundation (DFG) is conducted on this material at Material Testing Institute of Stuttgart University.

The aims of the project comprise the consistent experimental characterization and numerical modeling of the constitutive behavior of the material at static and quasi static cyclic loading. With regard to structures, the load carrying behavior of the board material, used as sheeting of seismically loaded timber frame shear walls, and its interaction with dowel type fasteners is investigated.

In the frame of the experimental material characterization and modelling, a profound understanding of the different stages of the softening mechanism is essential. So, for example present knowledge of the material behavior does not allow a judgement at what stage of the pre-peak loading path strain localization starts. Results from bending specimens did not reveal thus far whether the first nonlinearity stems from distributed micro-cracking localizing in the late stage into a crack band. However, it could also be that micro-cracking area is localizing from very early loading stages due to very high material inhomogenity at the mesolevel.

In order to identify the softening region directly in an advanced experimental approach, optical strain measurements were performed with a laser extensometer enabling a continuos locally resolved one-dimensional observation of the strain evolution within a globally relevant length scale. The employed experimental procedure allows a direct observation of the initially unknown locus of fracture localization and distributed micro-cracking within a zone of certain deliberate width. Complementary, the fracture appearance is also characterized by scanning electron microscopy aiming at a thorough understanding of the cohesion/decohesion features of the matrix fiber compound.

This article reports on first results obtained in uniaxial static tension tests with unnotched specimens.

2. SPECIMEN AND TEST SETUP

The material used was fiber gypsum board with a thickness of 12,5 mm conforming to product requirements specified in [4]. Figure 1a shows the geometry and the dimensions of the employed necked tension specimens.

The moisture content of the specimens at test time was 1,5% being typical for that material after conditioning at a climate of 65% relative humidity and 20°C.

For purpose of contact free optical strain measurement along the center part of the specimen with constant width of 30 mm, an optical grid was glued one-sided on the specimen as shown in Fig. 1b. The optical grid consists of black strips with a width of 1 mm arranged in a distance of 2 mm (center to center). During performance of the monotonic tension test, the transition of light (translucent) and black strips is scanned by a laser extensometer with a frequency of 50 Hz. The evaluation of strains between the individual strips of the grid is performed by differentiation of the relative changes of the grid distances. The tension tests were performed displacement controlled with a cross-head loading speed of 0,2 mm/min. The size of the specimen was chosen in such a manner that instable failure due to too high release of elastic energy from undamaged parts at unloading is avoided.

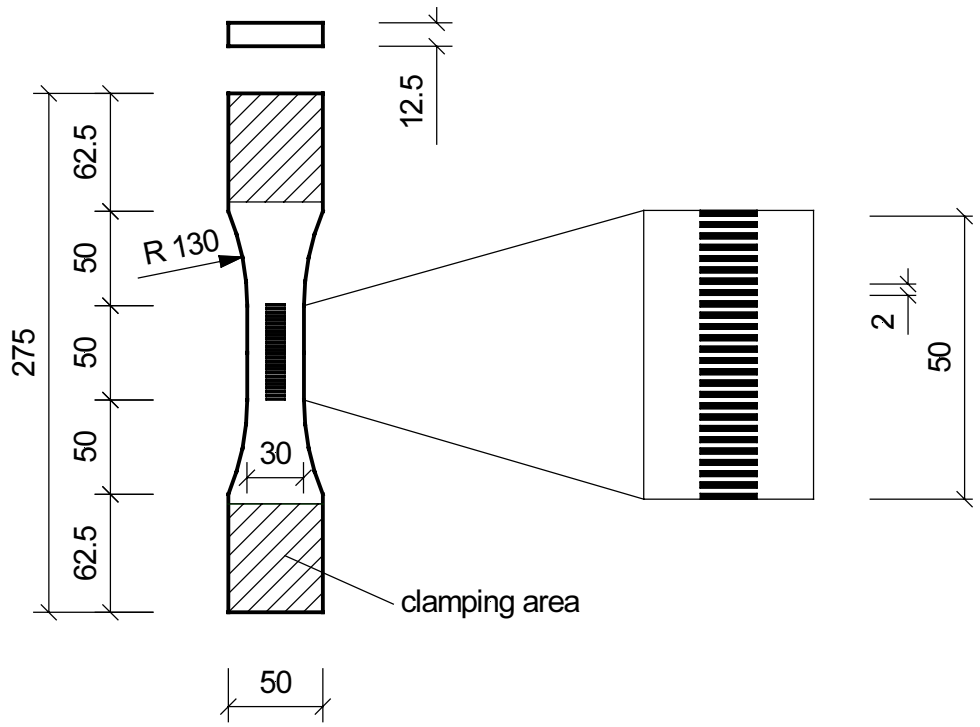

Fig. 1a: Specimen and test set-up

Fig. 1b: Optical grid

3. TEST RESULTS

3.1 Stress vs. mean strain relation

All following statements refer to the same specimen chosen as being well representative for the five specimens tested so far. Figure 2 shows two curves of tension stress σ vs. mean strain $\bar{\varepsilon}$ of the same specimen until complete fracture (note: mean strain $\bar{\varepsilon}$ is understood as the averaged strain within a certain distance). The given curves differ with respect to the total length L of strain measurement. One curve refers to $L = L_2 = 50$ mm, being the total length of the applied optical grid, whereas the other curve is related to $L = L_1 = 20$ mm. In both cases, the damage localization and fracture zone lies within distance L.

The difference of the depicted curves can be easily explained by a crack band or series coupling model [5, 6]. As shown subsequently, this simple model of strain localization applies very well for the material under consideration. In a crack band model, it is assumed that distributed fracture localizes in one segment of length h of the specimen whereas the rest of the specimen with length $L^* - h$ behaves in a linear elastic manner beyond peak load. In the model it is assumed that the strain state is roughly constant over the cross-section. Length L^* is the total free length of the specimen, which in the regarded case is larger than maximum length L of the optical grid.

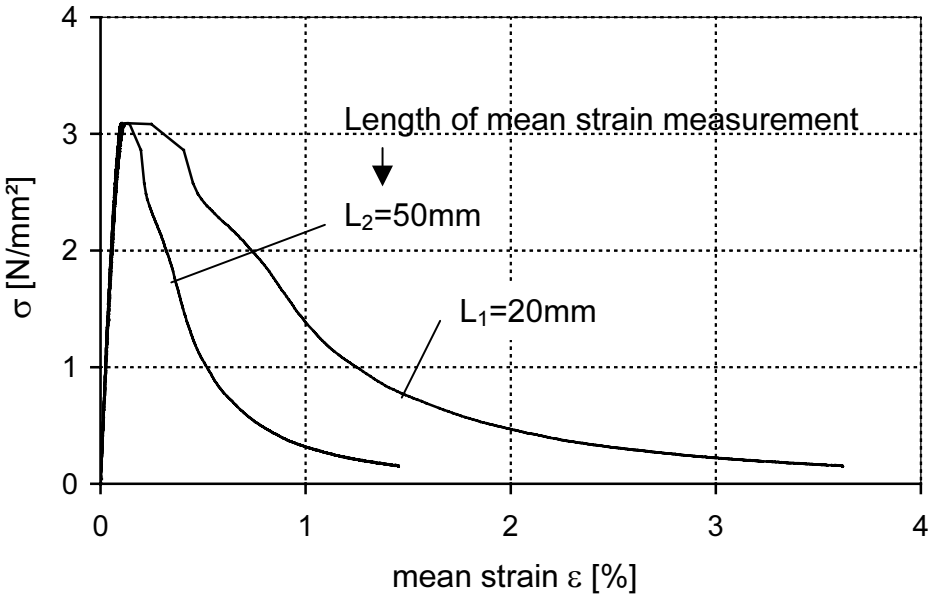

Fig. 2: Influence of length of mean strain measurement on global stress strain relation of fiber gypsum board including a crack band

Assuming a series coupling model it is obvious that strain energy density G_f/L, being the area under the loading and softening branch of the specimen´s $\sigma-\bar{\varepsilon}-$curve is considerably larger for mean strain measurement length L_1 as compared to L_2. Hereby, it is tacitly assumed that localization length h is smaller than L_1.

The fracture appearance of the tension crack shows a multiplicity of fibers sticking out of the matrix. Some fibers are broken, but predominantly fiber pull out occurs. Figure 3 exemplarily illustrates a fiber with good compound. However, large differences in the matrix-fiber interfaces were observed. One reason for this consists in the different fiber surface properties, as the fibers stem from a very heterogenous source of waste paper.

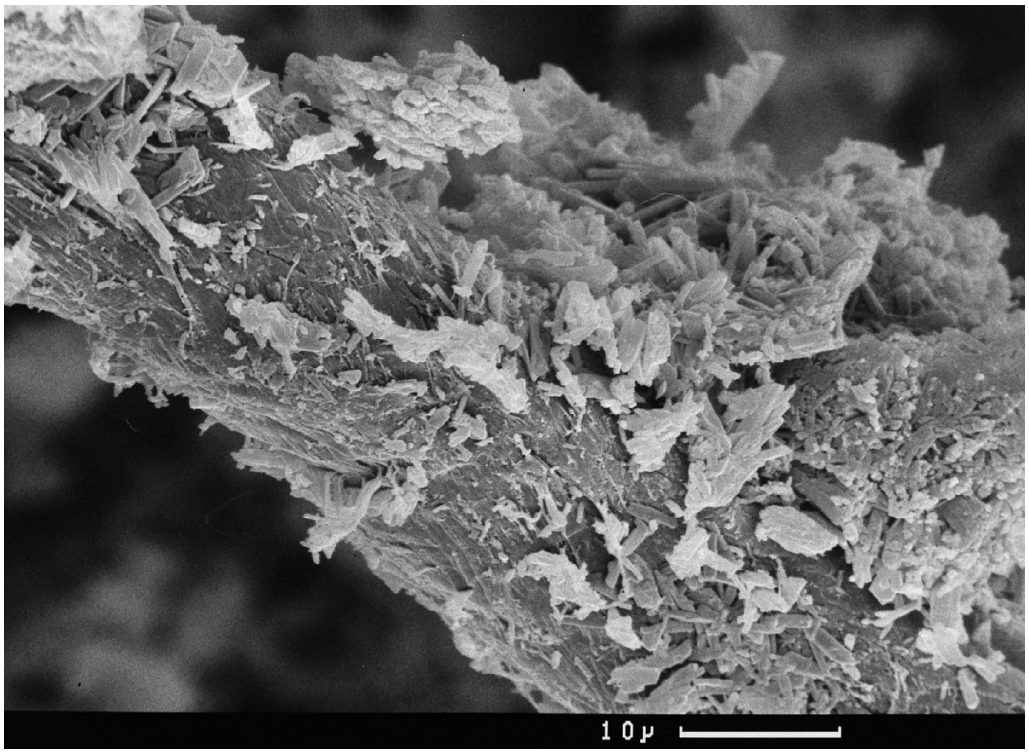

Fig. 3: Cellulose fiber with small gypsum crystals at the periphery

3.2 Strain localization

Figures 4a and 4b show the strain distribution along total strain measurement length of L = 50 mm at different global tension stress levels within the pre- and post-peak load range. The most interesting feature revealed in the graphs of the pre-peak regime is, that a very early, almost instantaneous strain localization (area of elevated strain) occurs; in Fig. 4a, this is shown for the lowest stress level of 0,5 N/mm^2. The width of the strain localization band grows by a factor

of 2 to 3 until ultimate stress; in the regarded example the ultimate capacity is denoted by a tension strength of $f_t' = 3{,}09$ N/mm^2. The crack band width h at f_t' is about 6 mm.

The post-peak strain distribution is given in Fig. 4b for three decreasing load levels of 2,5, 1,5 and 0,7 N/mm^2. The graphs reveal the expressed strain localization in the damage zone and the elastic unloading of the rest of the specimen. The width of the crack band increases in the post-peak regime to about 7 mm.

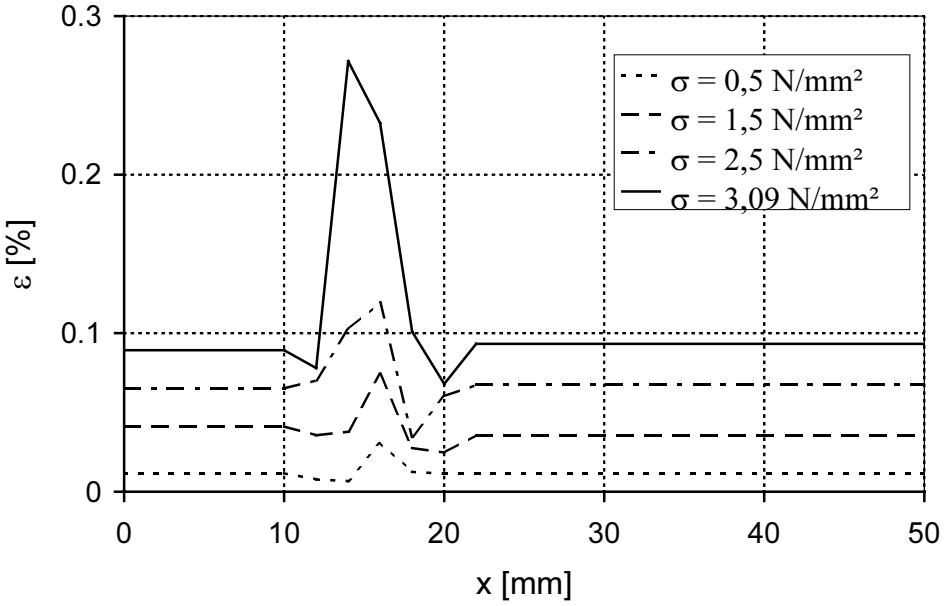

Fig. 4a: Strain distribution and localization at different stress levels in the pre-peak load regime

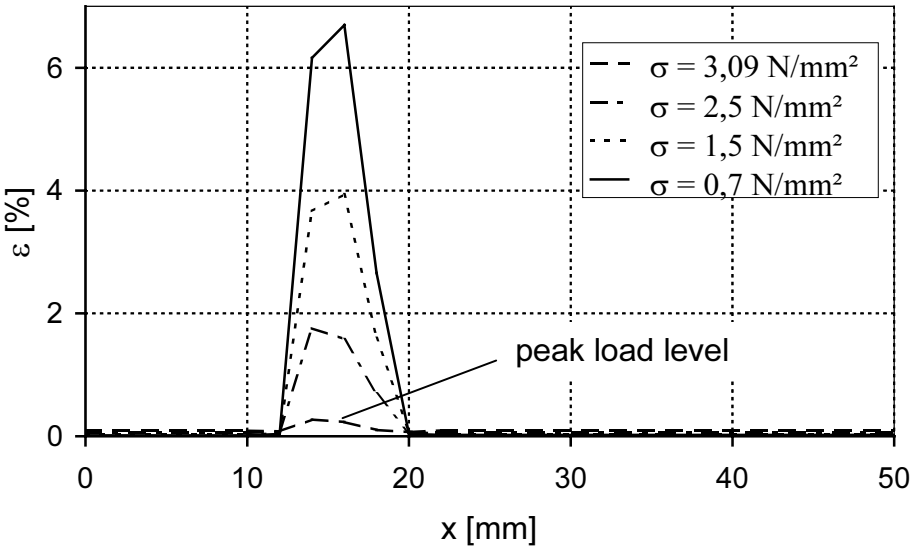

Fig. 4b: Strain distribution and localization at different stress levels in the post-peak load regime

3.3 Average unloading and softening moduli

Figures 5a and 5b show the constitutive behavior of the elastically behaving undamaged series model part (Fig. 5a) and of the damaged part with strain localization (Fig. 5b). In detail, Fig. 5a represents the averaged stress vs. mean strain relationship of length $L - h = 50 - 7$ mm. A very close matching of the loading and unloading branch is visible. The small damage/quasi-plasticity at peak load is disregarded in this first evaluation. In addition to the experimentally observed material behavior, Fig. 5a gives the averaged unloading modulus of elasticity, determined as

$$\overline{E_u} = 3870 \quad N / mm^2 .$$

Figure 5b gives the average $\sigma - \bar{\varepsilon}$ –relationship within the crack band width, here assumed to be 7,0 mm, as discussed in chap. 2.2. From Fig. 5b, the averaged softening modulus of elasticity is derived in a simplified linearized approach from equality of the actual and triangularized specific strain energy area as

$$\overline{E_t} = -52 \ N/mm^2 .$$

3.4 Fracture energy

Fracture energy G_f represents the released strain energy density

$$U = \int \sigma \, d\varepsilon \tag{1}$$

integrated over the volume resp. length (in case of unit area) of the assumed damage localization, i.e.

$$G_f = h \cdot \int \sigma \ d\varepsilon \tag{2}$$

This is visualized in Fig. 6. Assuming inequality of the elastic loading and unloading branch within the strain localization length, which in general is the case, fracture energy obviously is [6]

$$G_f = h \left(\int_{\varepsilon_1}^{\varepsilon_p} \sigma \ d\varepsilon + \int_{\varepsilon_p}^{\infty} \sigma \, d\varepsilon \right) \tag{3}$$

In the following, based on the minor differences of the elastic loading and unloading paths shown in Fig. 5a, eq. (2) is used for the determination of G_f. Employing the averaged unloading and softening moduli of elasticity, $\overline{E_u}$ and $\overline{E_t}$, derived

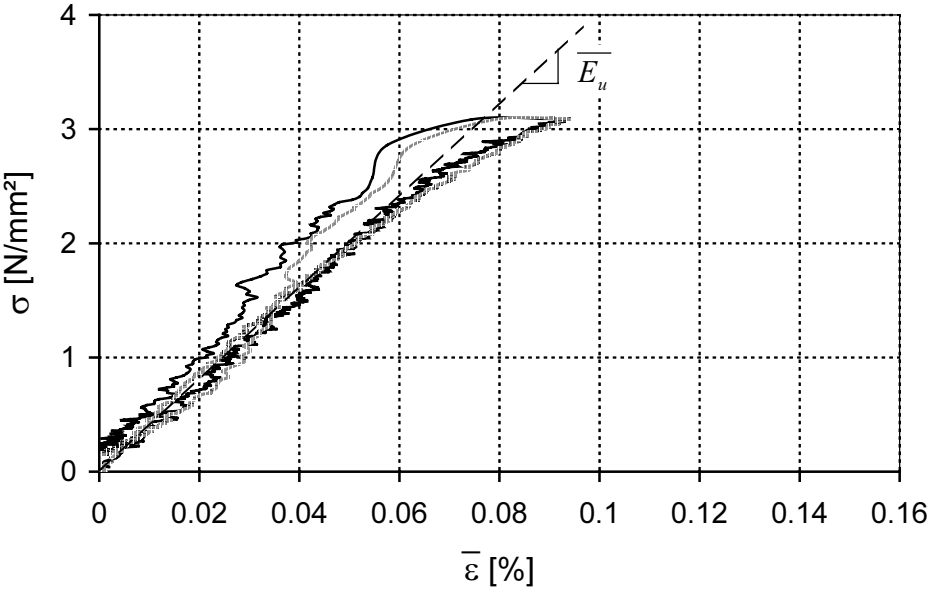

Fig. 5a: Averaged stress-strain-relationship of the undamaged elastic specimen zones

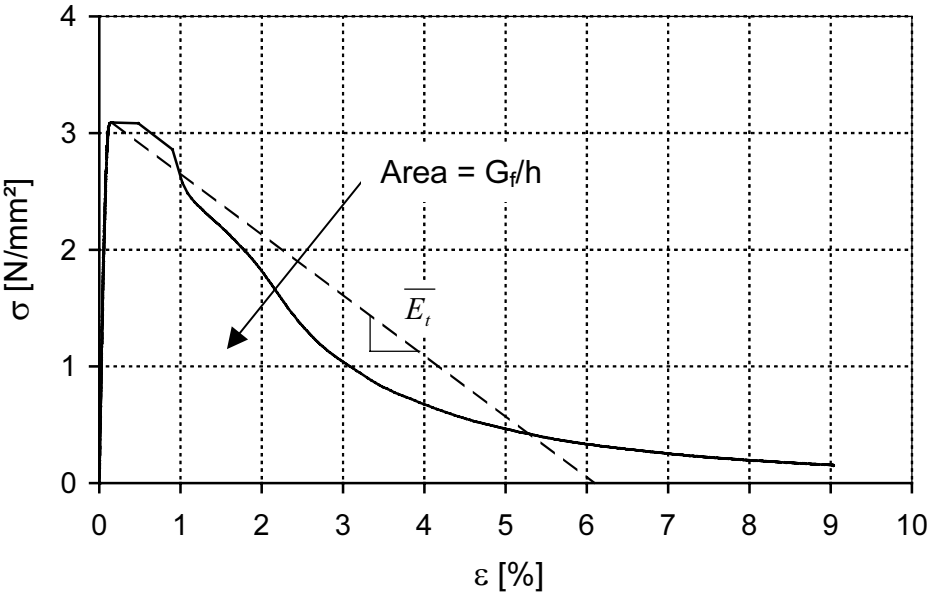

Fig. 5b: Averaged stress-strain-relationship of the softening zone

above, fracture energy can be expressed equivalently by eqs. (2) and (3) as

$$G_f = \frac{f_t'^2\, h}{2}\left(\frac{1}{\overline{\overline{E_u}}} - \frac{1}{\overline{\overline{E_t}}}\right) \tag{4}$$

For the specimen under consideration, strain energy density $U = G_f/h$, being the area under the $\sigma - \bar{\varepsilon}$–relationship in Fig. 5b is

$U = 0{,}0892\ N/mm^2$

Hence, fracture energy is roughly ($h \approx 7{,}0$ mm)

$$G_f = 7{,}0 \cdot 0{,}0892 = 620 \ N/m$$

Alternatively, when fracture energy is determined from eq. (4) a well conforming value of

$$G_f = \frac{3{,}1^2 \cdot 7{,}0}{2}\left(\frac{1}{3870} - \frac{1}{-52}\right) = 660 \ N/m$$

is obtained.

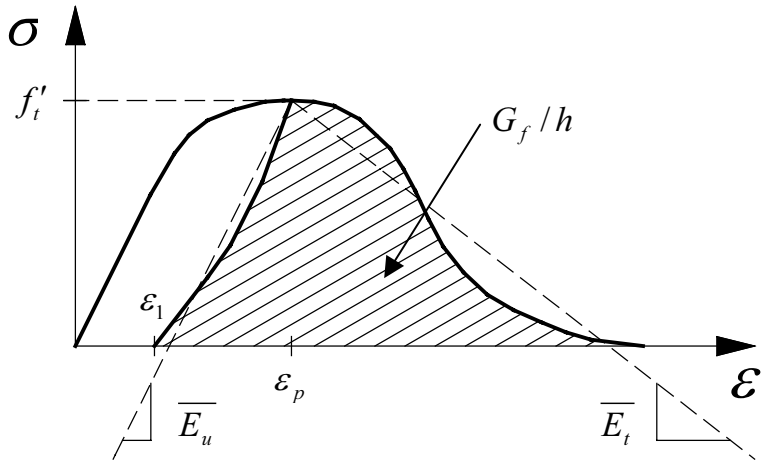

Fig. 6: Release of strain energy density within the crack band

Based on the idea of the crack band model with negligible fracture energy contributions from the parts outside the strain localization band, fracture energy can also be derived from strain energy density based on averaged strain $\bar{\varepsilon}$ within a deliberate length L (resp. within volume $L \times A$):

$$G_f = L \cdot \int \sigma \, d\bar{\varepsilon}_L \tag{5}$$

So, for instance, strain energy density obtained for $L = 50$ mm, i.e. from the area under the $\sigma - \bar{\varepsilon}$ −curve given in Fig. 2, is

$$U_L = \int \sigma \, d\bar{\varepsilon}_{50} = 0{,}0125 \ N/mm^2$$

and hence

$$G_f = 0{,}0125 \cdot 50 = 630 \ N/m$$

As can be seen, a rather good agreement between the various evaluation methods is obtained; this is valid for all specimens tested.

4. CONCLUSIONS

The performed investigations revealed the good applicability of the employed experimental setup for monitoring of strain localization into a damage band of tension loaded fiber gypsum board material. The contact free laser extensometer based strain measurements allow the quantitative separation of stress and/or time dependent strain evolutions in the a priori unknown location of the damaged material zone and the adjacent undamaged parts. The resolution accuracy, being at present 2 mm, allows a sufficiently accurate determination of the crack band width of the regarded fiber gypsum composite material.

Complementary fracture surface imaging by means of electron microscopy revealed one major explanation for the expressed softening characteristics of the material built up of two brittle components, being gypsum and paper fiber: this is bound to the partly very low fiber matrix compound.

Preliminary results of ongoing investigations with quasi static cyclic loading of joints of the material with dowel type fasteners show that joints are characterized by considerable ductility / energy dissipation capacity resulting especially, however not exclusively from the described softening behavior in tension loading. This should qualify the material for bracing of timber frame shear walls subjected to seismic impacts.

ACKNOWLEDGEMENTS

The authors gratefully acknowledge the financial support of the research work by a grant from the German Research Foundation (Deutsche Forschungsgemeinschaft – DFG) to Special Research Area (Sonderforschungsbereich – SFB 381), and hereby to thematic subproject A11 “Damage of structures made of cellulosic short fiber composite materials”. Sincere thanks are indepted to Dr. Patrick Castera, Director of LRBB (Laboratoire de Rhéologie du Bois de Bordeaux) for providing the French abstract.

REFERENCES

[1] AICHER, S., KLÖCK, W. (2000): *Fracture modeling of wood fiber gypsum board.* Proceed. Int. Conf. on Wood and Wood fiber Composites, pp. 469 – 480, Otto-Graf-Institut, Stuttgart

[2] KLÖCK, W., AICHER, S. (2005): *Size effect in paper fiber-reinforced gypsum panels under in-plane bending.* Wood and Fiber Science, in press

[3] AICHER, S., KLÖCK, W., REINHARDT, H.W. (2004): *Fracture properties of wood fiber gypsum boards form size effect.* Submitted to ASCE, J. Eng. Mechanics

[4] N. N. (2003): *German technical approval Z-9.1-434.* Deutsches Institut für Bautechnik, Berlin

[5] BAŽANT Z. P., OH, B. H. (1983): *Crack band theory for fracture of concrete.* Materials and Structures (RILEM, Paris), 16: 155 - 177

[6] BAŽANT, Z. P., CEDOLIN, L. (1991): *Stability of Structures. Elastic, Inelastic, Fracture, and Damage Theories.* Oxford University Press